Desalination and Water Treatment
www.deswater.com

doi: 10.5004/dwt.2021.27697

236 (2021) 250–263
October

Synthesis of Cu/Zn doped zeolite hybrids for batch remediation of toxic environmental pollutants

Noshabah Tabassum[a,*], Uzaira Rafique[b]

[a]*Department of Environmental Sciences, Fatima Jinnah Women University, The Mall, Rawalpindi 46000, Pakistan, email: noshabah.khattak@gmail.com*
[b]*Deans Faculty of Science and Technology, Fatima Jinnah Women University, The Mall, Rawalpindi 46000, Pakistan, email: uzairaiqbal@yahoo.com*

Received 3 February 2021; Accepted 4 August 2021

ABSTRACT

The industrial revolution has led to an unequal and uncontrolled distribution of the toxic substances in different environmental compartments. A large number of researchers have offered specific solution to combat the hazardous and toxic substances. The real challenge faced today is the complex interaction of the pollutants in each compartment compelling the scientists to develop materials offering one spot solution applicable to a wide range of toxicants. In the present research, zeolite as base material is synthesized from economical precursors using hydrothermal method. Post modification for synthesis of functionalized hybrids is attempted with doping of metals (Cu, Zn). The purpose of preparation of hybrids is to have diverse functional groups on the surface of a single zeolite to adsorb a variety of pollutants from environmental media. The synthesized materials are subjected to a series of characterization techniques [Fourier-transform infrared spectroscopy (FTIR), X-ray diffraction (XRD), thermogravimetric analysis (TGA), scanning electron microscopy/Energy-dispersive X-ray (SEM/EDX)] to determine surface and bulk properties for effective adsorption. The successful incorporation of metal-oxygen is indicated by FTIR. SEM analysis proposes that crevices and channels serve as pores for uptake of incoming pollutants. Further, EDX shows silica and alumina percentage which is involved in developing zeolite framework (internal and external linkages) for binding. The thermal stability of zeolite (360°C–570°C) is assessed from TGA studies. XRD demonstrates the amorphous nature of zeolite framework that generally decreases on functionalization. Zeolite and the functionalized hybrids are applied for the removal of metals (Hg, As), dyes (Methylene blue, Methyl orange). Generally, mercury showed better removal than arsenic on the adsorbents. Moreover all zeolite based hybrids testifies the fitness of pseudo-second-order kinetics and Langmuir and Freundlich isotherms for the removal of mercury and arsenic.

Keywords: Zeolite; Precursors; Hydrothermal method; Hybrids

1. Introduction

The environment today has become very complex and contaminated with different pollutants. The air is loaded with gaseous pollutants, the water used for drinking; washing, agricultural and industrial purposes have metals, dyes, and pesticides residues. Furthermore, these pollutants produce a considerable waste, adding to the cost for waste management and environmental health. The industrial revolution has led to an unequal and uncontrolled distribution of the toxic substances in the environment. Exposure to these pollutants through intake of plants derived foods and beverages, drinking water or air exerts short and long term effects on human health [1–3]. For instance, arsenic

* Corresponding author.

contamination in water is linked to skin cancer, arsenical dermatitis, neurological effects, liver enlargement and heart diseases [4,5]. Similarly, exposure to mercury cause impairment of pulmonary and kidney function and also promotes tyrosinemia [6]. Heavy metal pollution is increasing day by day calling for immediate remediation actions. Many industries such as metal plating, mining, fertilizers, paper, pesticides, batteries, etc. are directly discharging their heavy metal wastewater into environmental compartments. These pollutants are non-biodegradable so they tend to accumulate in living organisms through food chain [7]. Most of these metals such as mercury, lead, arsenic and chromium are classified as carcinogenic [8]. The most deleterious effects are integrated by mercury and arsenic because of high toxicity, volatility, bioaccumulation capacity and persistence for longer duration in the environment. The discarded fluorescent bulbs, electrical fixers, switches, medical equipment's and thermostats etc. are main sources of mercury contamination. The mercury in organic form is more obvious, whereas inorganic forms can be biologically methylated showing high tendency for bioaccumulation [9]. A rigorous control in a cost-effective manner is required for leaching of mercury from wastewater sources [10]. Clean-up technologies are capable of treating large volumes of soil, water or sediment contaminated with relatively low levels of mercury.

Arsenic, the most abundant element in the earth crust, exhibits complex chemistry due to several oxidation states. The sources of arsenic in environment are mostly geological formations such as volcanic rocks, sediments etc. [11] from where it can leach as soluble metal into ground water [12]. However anthropogenic sources and products such as wood preservatives, semi-conductors, and agricultural appliances are also responsible for arsenic pollution [13]. Although arsenic is found in several forms in food and environmental compartments, but in drinking water it is highly toxic. The maximum contaminant level for arsenic in drinking water is 10 μg/L (World Health Organization, 2004).

The identification of heavy metals in different environmental compartments is a serious challenge because of their increase discharge, toxicity and other negative effects in receiving compartment. Removal of metal ions from wastewaters is one of the most important areas of research. The pre-requisites of selected removal technique for metal ions are safe operation, low cost, high efficiency and easy handling [14].

Azo dyes are an important group of xenobiotic compounds that are recalcitrant to degradation processes. The colored dyes generated by the textile, printing, plastic and paper making industries pose a serious threat to environmental and public health [15]. Even the small amounts of dyes in industrial wastewater are highly visible and undesirable [16,17]. The colored water generated by the textile industry is rated as the most polluting among all industrial sectors [18].

The commonly employed dyes in printing, textile, food, pharmaceutical, paper, wood and research laboratories [19,20] are Methyl orange (MO) and Methylene blue (MB). The toxicity of both dyes is well established. Furthermore, dye materials are not easy to degrade because of their high stability to light and oxidation reaction [21].

The genotoxic and mutagenic effects in humans [22] are reported by the release of azo-dyes from textile, pharmaceutical and printing industries. A large number of researchers have offered solution to combat the pollution problems and each solution has a certain degree of specificity. Considering the scenario where a single environmental compartment cannot stand alone, efforts are required to be directed towards a single solution to multi-problems.

Although a number of materials and techniques have been utilized, the use of zeolites and their modified forms offer advantages such as low-cost, ease of availability, good mechanical and thermal properties and high sorption capacity. Zeolites represent an important group of materials and have attracted ever-increasing interest from academic and industrial laboratories due to high catalytic and exchange properties. Their application as cation exchanger for removal of heavy metal is described in the literature for water and industrial waste treatment [23–25]. For instance, a molecular complex sorption mechanism is expected [26] in the case of arsenic. The exchange between terminal aluminol or silanol hydroxyl groups and adsorbate anionic species results in arsenic adsorption at the edges of the zeolite particles [27,28]. A significant expansion in the area of application can be made by functionalization of the zeolite surface [29].

Metal functionalization is an essential tool to tailor the physicochemical properties of already synthesized zeolites. The first modification process is reported in the late 1960s, with significant advances in early 1980s [30]. The metal incorporation is helpful to enhance the adsorption, catalytic and shape selective properties. For this purpose, different post synthesis multistep protocols like ionic exchange [31,32], impregnation [33], or chemical vapor deposition [34] is reported. The incorporation of metal improves the framework topologies [35] and attains good dispersion without disturbing the structure stability [36,37] of zeolites. The metal functionalized zeolites show remarkable application like ion exchange, catalytic activity [38] and redox catalysts, due to tetrahedral isolated metal atoms into the molecular sieve framework which can undergo changes in their oxidation state. For instance, these materials are used in oxidation of benzene to phenol [39] [24], oxidation of methane to methanol [40], oxidation of ethane to oxygenate [41] and catalytic reduction of NO [42]. More specifically, Cu and Fe modified forms are successfully utilized for pollution problem because of their precise microporosity, strong acidity and high thermal stability [40,43].

The scope of this work is to conduct the synthesis and characterization of zeolites using both reported and novel methods, enhancing their potential applications for environmental remediation by functionalization with metals. Evaluated applications include the efficiency of both zeolites and their hybrids for removal of contaminants from polluted effluents as potential remediation alternatives.

2. Experimental

2.1. Chemicals

Sodium silicate (Na_2SiO_3), aluminium isopropoxide ($C_9H_21AlO_3$), sodium hydroxide (NaOH), copper

nitrate $Cu(NO_3)_2$, zinc nitrate $Zn(NO_3)_2$, Methyl orange ($C_{14}H_{14}N_3NaOS$), Methylene blue ($C_{16}H_{18}ClN_3S$) are procured from Sigma-Aldrich and used without purification.

2.2. Characterization

Each of the synthesized zeolite and its metal functionalized hybrids are characterized by an extensive range of techniques like Fourier-transform infrared spectroscopy (FTIR), scanning electron microscopy/Energy-dispersive X-ray (SEM/EDX), X-ray diffraction (XRD), thermogravimetric analysis (TGA) and Brunauer–Emmett–Teller (BET) to find out their surface and bulk properties.

FTIR is an analytical technique that identifies the functional groups of materials. In this research, the pressed KBr pellets of the synthesized zeolites are subjected to FTIR spectrophotometer (FTIR 8400, Shimadzu, Japan) to determine the functional groups likely to contribute in binding of the materials. Each material is independently run on FTIR and a spectrum is recorded. SEM/EDX. Scanning electron microscopy (Quanta 200 FEI) operated under 10 kV voltage and distance of 10 mm. The sample was sputtered with gold to prevent sample charging and placed on a thin film of carbon tape mounted on stub. Air pulse was applied to remove excess and loose sample and then placed inside a vacuum chamber under argon.

XRD is non-destructive technique primarily used for phase identification of a material in which X-rays are generated and impinged on target material to dislodge inner shell electrons. The diffraction pattern for zeolite and its hybrids were recorded using Bruker D8 X-Ray Diffractometer having Cu-Kα radiation (1.54056 Å) with 0.02 step size from 5° to 80°. Thermogravimetric analysis (Mettler Toledo AG) was used to measure the change in mass of a sample as a function of temperature under nitrogen.

2.3. Procedure for synthesis of zeolite framework (Z)

In the present investigation, the zeolite framework is synthesized following the reported protocol [44]. An equimolar ratio of sodium silicate (5 g) and aluminum isopropoxide (5 g) is dissolved in alkaline medium (2 M NaOH). The mixture is continuously stirred at room temperature till complete dissolution. The homogenized mixture is autoclaved at 121°C for 4 h. The crude white product obtained is washed in detail with deionized water and dried in oven for 12 h at 110°C. The product is coded as Z (zeolite framework).

2.4. Procedure for the synthesis of metal functionalized zeolites

The procedure layout follows addition of individual metal solution of zinc nitrate and copper nitrate into synthesized zeolite. The mixture is thoroughly stirred at 400 rpm for 6 h and temperature is maintained at 70°C. The crude products are washed and dried. Two metal functionalized hybrids are synthesized and coded as ZC and ZZ.

2.5. Environmental remediation application

The base material zeolite (sample Z) and metal functionalized hybrids are opted for a wider application window. The applications include removal of Metals (Hg, As) and removal of dyes (Methylene blue, Methyl orange). For each application, closed batch adsorption protocol is followed.

The synthetic solution of Hg and As is subjected to batch removal using zeolite and its functionalized hybrids. The stock solution of metal ions with the concentration of 1,000 mg/L is prepared and dilution of 0.1 mg/L is made with distilled water. The batch experiment is conducted by taking adsorbent dose (5, 10, and 15 mg) in solution of 0.1 mg/L. The solution is placed for 30 min on shaking at 150 rpm. An aliquot is drawn after every 3 min, filtered and analyzed on AAS (Varian Spectra AA 220). Removal of metal (%*R*) by the zeolite and its functionalized hybrids is determined from Eq. (1).

$$\%R = \left(\frac{C_i - C_t}{C_i}\right) \times 100 \tag{1}$$

3. Result and discussion

3.1. Fourier-transform infrared spectroscopy

The wavenumbers recorded in the spectral region of 400–1,400 cm^{-1} indicated vibrations for the basic framework of zeolite (sample code Z). The band at 420–500 cm^{-1} is assigned to T–O bends, where T is Si or Al. More specifically, the silane (Si–H) linkage is observed at 2,300–2,360 cm^{-1}. The interaction of alumina tetrahedral and SiO_2 groups in zeolite framework is witnessed from 500–650 cm^{-1} also reported by [45], whereas peaks between 1,500–1,700 cm^{-1} are related the bending vibration of the adsorbed water molecules [46]. The presence of silica, alumina and water as components of single material (sample Z) clearly indicates successful conversion of basic ingredients into hydrated aluminosilicate defined as 'zeolite' (Fig. 1). Further, the presence of free water molecules in zeolite framework [47] is also witnessed by sharp and weak bands between 3,200 to 3,600 cm^{-1}.

The zeolite (sample Z) is subjected to metal doping for functionalization of zinc (sample ZZ) and copper (sample ZC) and the bimetallic functionalized hybrid (sample ZCZ) are characterized by FTIR spectroscopy.

FTIR spectrum of sample ZZ showed interesting vibrations. The absorption band at 418 and 889 cm^{-1} is characteristic of Zn–O [48] and Zn–O–Zn linkage, respectively. Another sharp absorption band at 434 cm^{-1} is observed corresponding to Zn–O vibration [49]. This confirms the successful doping of metal in zeolite (Fig. 1c). The metal-oxygen frequencies observed are in accordance with literature values [50–52]. The peak at 1,633 cm^{-1} correspond to Zn-O stretching, whereas the absence of deformation vibration peak around 620 cm^{-1} suggests that incorporation of Zinc has not changed the morphological character of amorphous zeolite [53]. Absorption peaks at 3,585 and 3,470 cm^{-1} are attributed to stretching vibration of free O–H bond, whereas bending vibration of H–O–H bonded water molecules are likely masked by the incorporation of zinc. The peaks observed were found comparable with earlier reports [54]. The interaction of zinc with zeolite constituents can further be explained by the broadening

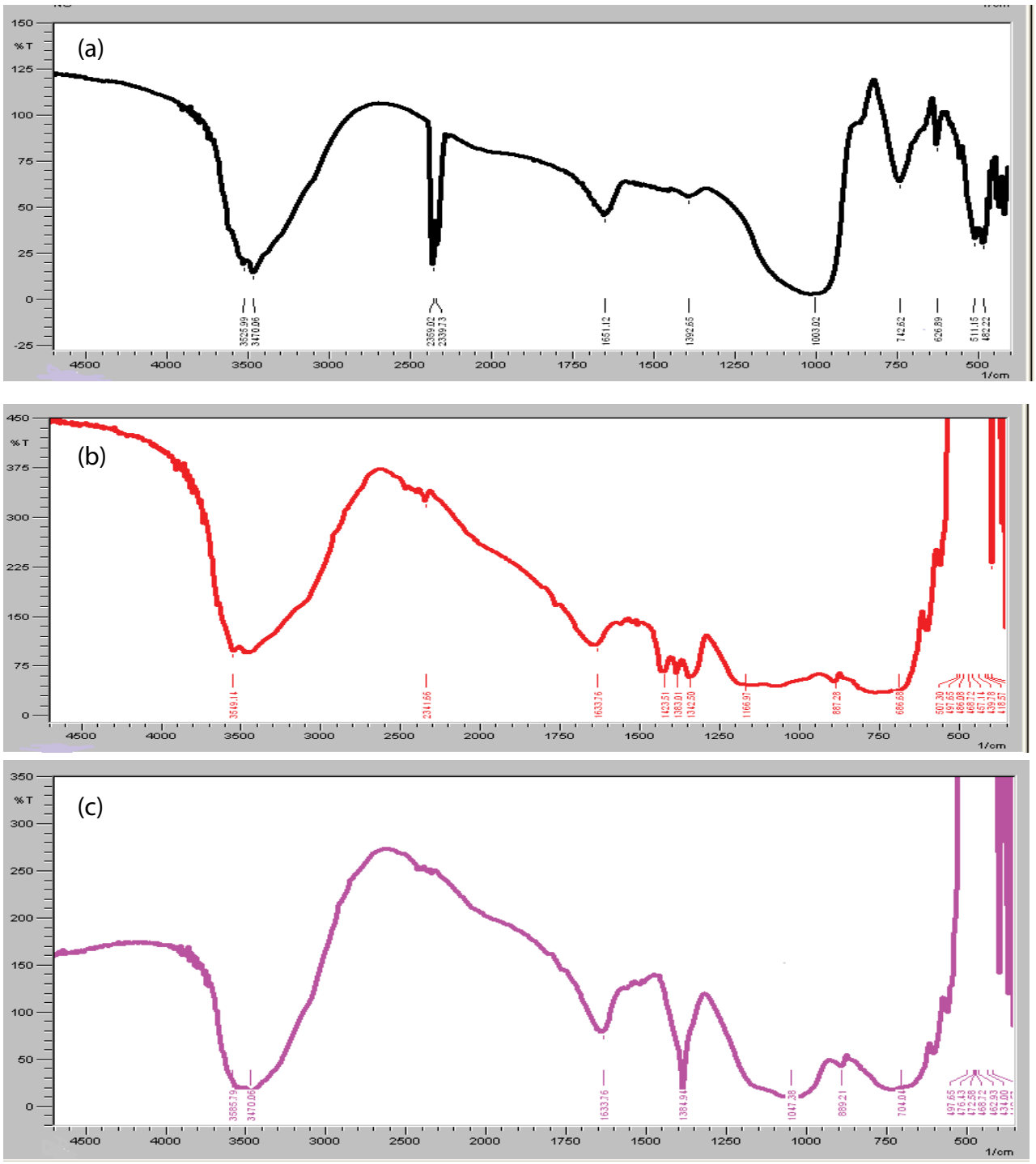

Fig. 1. FTIR spectra of zeolite and metal functionalized hybrids: (a) Z, (b) ZC, and (c) ZZ.

of asymmetric stretching of Si–O–Si (around 1,003 cm^{-1}) upon doping of respective metal indicating successful functionalization. Such changes are also observed in tin substituted ZSM-5 [55] and manganese substituted ZSM-5 [56]. However, relative to zeolite framework, minor peak shifting is noticed in zinc doped zeolite. This suggests that zinc has been immobilized indicating changes in the cros-structural features of the zeolite framework [57].

FTIR spectra of Cu-doped zeolite can be distinguished from Zn-doped zeolite by the emergence of ring vibration and Silane in the former (Fig. 1b). In addition, the peculiar, Cu–O symmetric and Cu–O asymmetric stretching observed at 439 and 507 cm^{-1} confirms the formation of copper functionalized zeolite [58]. The metal–oxygen bond at 1,383 cm^{-1} (M–O rocking in plane) and at 1,633 cm^{-1} (M–O rocking out of plane) [59] indicates formation of CuO from copper

salt. However, an intense band at 1,633 cm^{-1} further suggests that copper is localized in extra framework positions. Other weak peaks may correspond to the impurities in the zeolite framework.

3.2. Scanning electron microscopy analysis

Each of the synthesized zeolite is scanned under electron microscope to figure out the morphological features. The aggregation of silica and alumina in the zeolite (base material) with wider channels is visible in Fig. 2a. On the contrary, the metal doped zeolites exhibited filling up of the spaces with relatively less void spaces. Further, the developed linkages of metal with Si/Al content are visible as fine intricate connectivity between the two. Relatively higher Si:Al in Zn-doped zeolite (also witnessed in EDX) suggest more close contact and deeper crevices in comparison to wider slits in Cu-doped zeolite. It is expected that earlier (Zn-doped) inorganic functionalized hybrid will be a relatively better adsorbent than later (Cu-doped).

3.3. Energy-dispersive X-ray analysis

Electron dispersive X-ray spectrums are obtained coupled with SEM images. It is noticed that each synthesized zeolite has a major component of silica and alumina. The results are given in Fig. 3. The zeolite represents the basic ingredients of Silica and Alumina in the ratio of 1:1.34 (15.09%:11.23%) in respective order. The higher (56.46%) oxygen and minimal (2.27%) carbon content suggests the presence of silicon-aluminum as oxides and inorganic composition of the zeolite.

3.4. Thermal gravimetric analysis

Each of the synthesized zeolite was subjected to thermal analysis to determine the degradation pattern as a function of temperature. It is generally observed that multistep degradation path is undertaken by each zeolite. The initial degradation is at relatively lower temperature.

The TG data is summarized in Table 1. It can be seen that zeolite framework has weight loss of only 13% up to 380°C. Further, a larger fraction of synthesized zeolite does not undergo thermal degradation. This is evident by the presence of more than 86% residue of the material. The thermal analysis concludes that synthesized zeolite is a thermally stable product and can withstand higher temperatures.

The thermal studies of hybrid functionalized zeolites with metals revealed interesting results. It is noted that

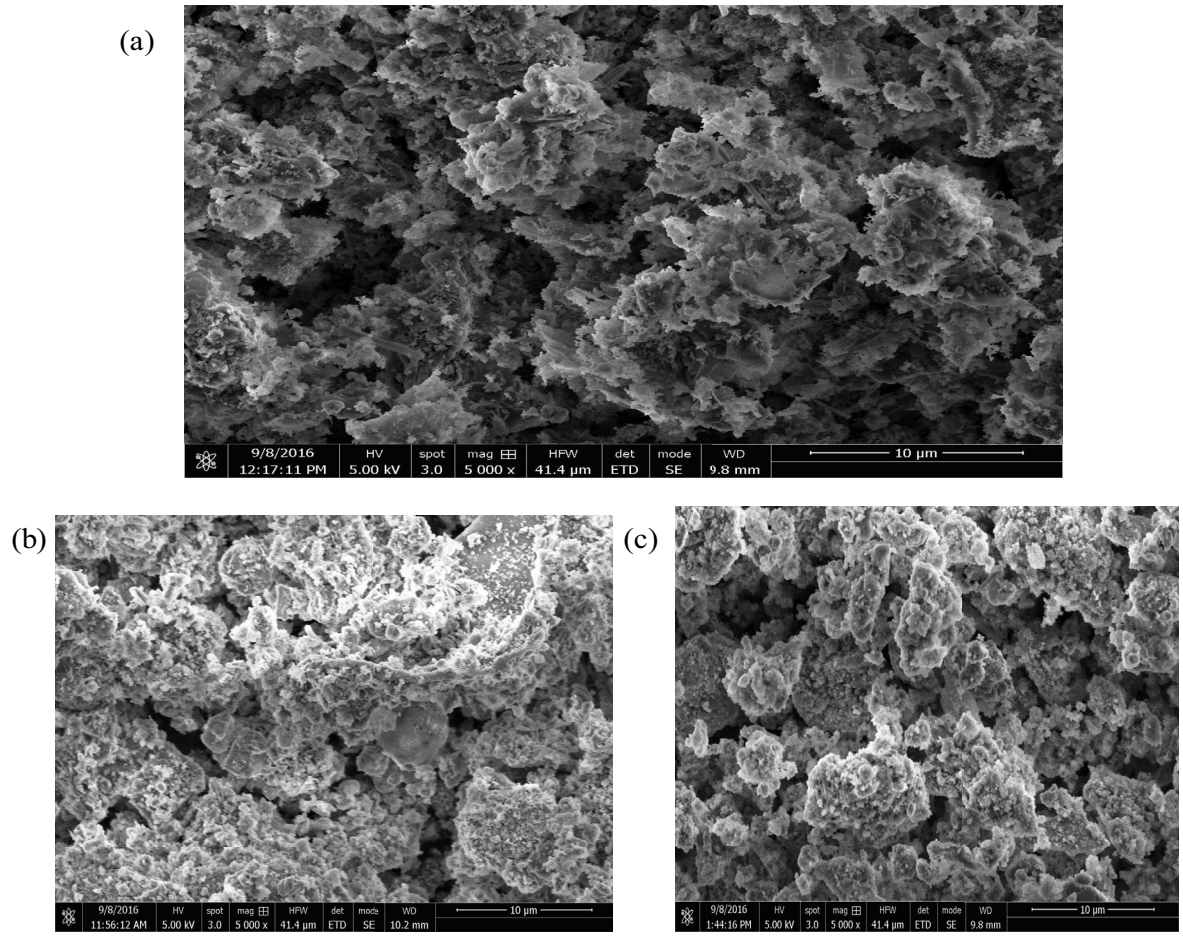

Fig. 2. SEM of zeolite and metal functionalized hybrids: (a) Z, (b) ZC, and (c) ZZ.

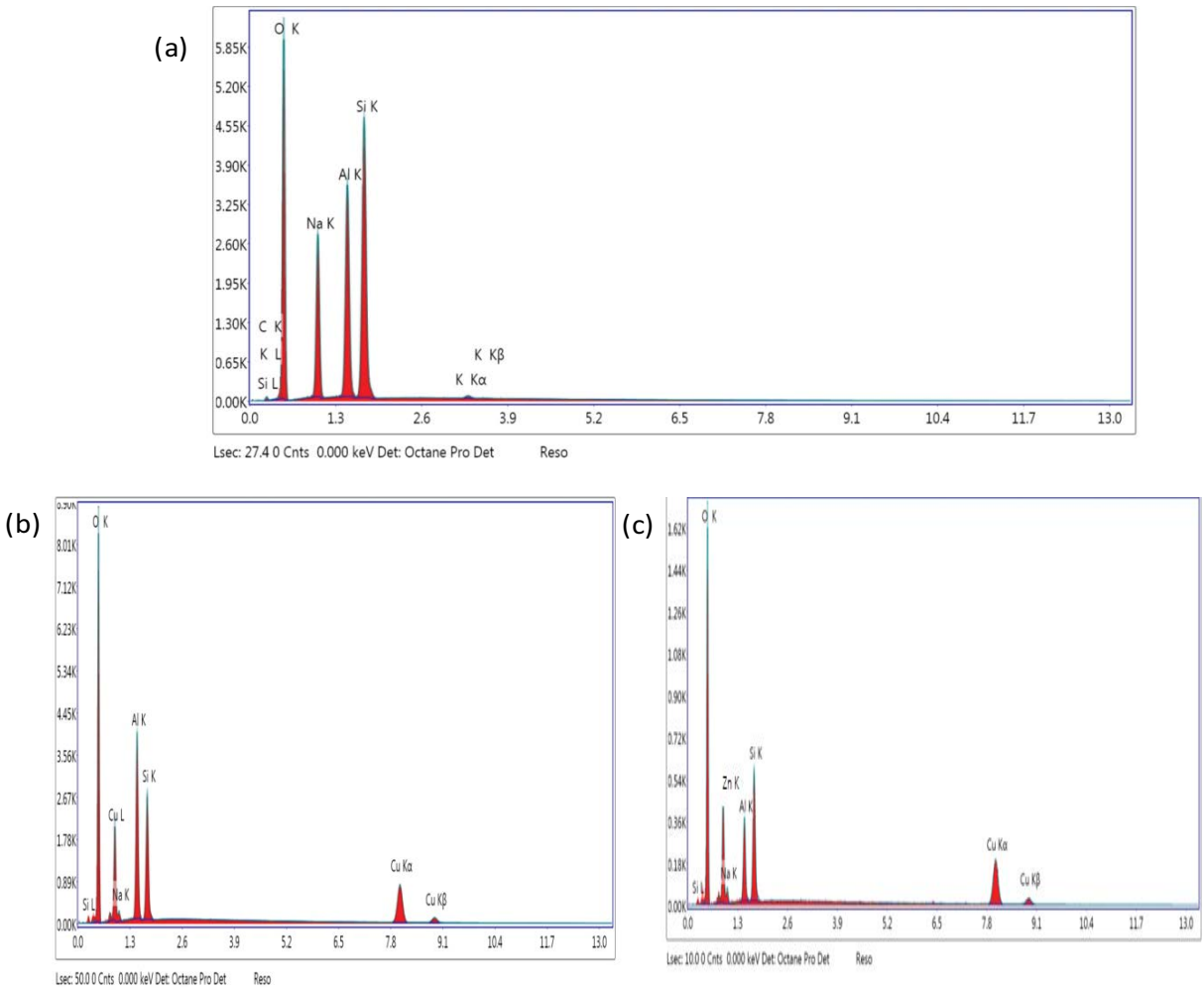

Fig. 3. EDX of zeolite and metal functionalized hybrids: (a) Z, (b) ZC, and (c) ZZ.

generally the introduction of a metal dopant into the base material zeolite has a relatively destabilizing effect.

The general observation noted for all of synthesized materials reveal that the initial weight loss at relatively lower temperatures is due to loss of solvent adsorbed (hydration water) on the surface of zeolite. In some cases, water is gradually removed [60] over a wider temperature range. On the other hand, thermal degradation at higher temperature (up to 400°C) can be attributed to modification due to induced doping effect in the zeolite structure. Similar behavior is also reported by [61]. Further, initial slower weight loss followed by relatively second significant loss may be caused by oxidation of organic group, dehydroxylation of the zeolite [62] or changes in overall composition of the framework.

The TG studies of all the synthesized zeolite materials follow the thermal stability sequence as:

Z > ZZ > ZC

The data of 50% decomposition presents the thermal studies as a function of temperature. The temperature at which 50% of the synthesized zeolite materials are degraded is tabulated and shown in Table 1. It is noted that higher temperature is required to decompose 50% of the material in case of metal doped zeolites. This is understood that metals exhibit extremely higher melting points than the organic component. The decomposition sequence of synthesized zeolites with respect to decomposition temperature is almost contrary to mass change. The thermal stability pattern is attributed to the zeolite structure [63].

3.5. X-ray diffraction analysis

In order to find out the amorphous or crystalline nature of the synthesized zeolites, X-ray diffractogram is obtained for each material (Appendix X) and the data is presented as angle of diffraction (2θ), d-spacing and relative intensity in Table 2.

The synthesis of silica alumina hydrate (zeolite) following hydrothermal method clearly demonstrates the amorphous nature of the material. On the other hand, zeolite doped with metals (Cu and Zn), increases the crystallinity. This suggests that large void spaces of amorphous zeolite are sequentially filled with the metal salt solution and the more uniform phase change occurs due to doping.

Table 1
Thermal analysis of zeolite and its metal functionalized hybrids

Sample codes	Step I: Loss (wt.%)	Step II: Loss (wt.%)	Total loss (wt.%)	Residue (wt.%)	Temperature (°C) at 50% decomposition
Z	5.5	8	13.5	86.5	368
	0°C–135°C	135°C–380°C			
ZC	10	18	28	72	230
	0°C–220°C	220°C–480°C			
ZZ	13	9.5	22.5	77.5	215
	0°C–265°C	265°C–525°C			

Table 2
XRD data of zeolite and its functionalized hybrids

Sample code	Pos. (°2Th.)	d-spacing (Å)	FWHM (°2Th.)	Rel. Int. (%)
Z	13.8	6.41	–	88
ZC	12.92	6.84	0.09	10
	18.83	4.71	0.47	7.98
	25.83	3.44	0.13	47.87
	36.64	2.45	0.19	33.51
	43.67	2.07	0.23	21.28
	62.81	1.47	0.57	6.91
ZZ	50.20	1.81	–	88
	53.25	1.71	–	98
	59.45	1.55	–	86

However, the frequency of sharp intense peaks is relatively more in Cu-doped than zinc-doped zeolite indicating more crystallinity in the former case.

3.6. BET surface area and particle size analysis

BET nitrogen gas adsorption method is usually used to determine the exact surface area of a material. Each of the synthesized material is degassed at 120°C for 60 min prior to measurement. The results are summarized in Table 3. It is interesting to note that each of the functionalized hybrid has relatively smaller particle size than the base material zeolite. This shows that doping of each functional group into the porous material has a stabilizing effect through filling up the vacant spaces available. The interaction between the zeolite and induced moiety helps in the development of relatively stronger linkages through physical forces. It is proposed that the inward pull is operative in functionalized hybrid thus reducing the particle size. The general sequence of particle size is as follows;

ZZ > ZC > Z

The BET surface area is another good parameter to assess the adsorption potential of the synthesized materials. It is generally observed that larger is the surface area, more adsorption results as adsorption is known to be a surface phenomenon. The doping of zinc in comparison to copper has increased the surface area likely due to d10 configuration of zinc in the periodic table. Zinc has strong binding affinity due to stable oxidation state so it does not require stabilization energy for ligands and other related stereochemical requirements. So as a result of strong binding affinity doping of zinc is more in comparison to copper. It can be concluded in general that porosity and larger surface area are contributing factors towards good adsorption potential.

Table 3
BET surface area and particle size of zeolite and its metal functionalized hybrids

Hybrids	Sample code	Particle size (μm)	BET surface area (m^2/g)
Zeolite basic framework	Z	24.38	14.727
Metal functionalized hybrids	ZC	15.39	28.684
	ZZ	9.027	66.084

3.7. Removal of metals

The toxicity of mercury and arsenic is well established. Removal of these metals from the compartments of water, soil, air, vegetation etc., is extensively explored. The present investigation is an attempt to propose remediation model for these metals using zeolite and its metal functionalized hybrids as adsorbents.

The study design involves application of each synthesized zeolite as independent adsorbent. The removal efficiency is measured as a function of time (up to 30 min) with three adsorbent dosages. The results are graphically presented through Figs. 4 and 5. Time has an important contribution in defining the removal capacity of the adsorbents. The base material zeolite (Z) served as a reference material for adsorption of mercury and arsenic. It is generally noted that adsorption increases with increase in time to optimum level followed by decrease in adsorption. This trend is observed in a number of adsorption studies [64] likely due to availability of empty sites initially on the surface of material leading to optimal saturation followed by emptying of spaces and discharging into the solution. Another aspect of this up and down adsorption trend is a closed batch system in which the adsorbent remains in contact with the solution for the entire duration of the experiment.

The adsorption studies conclude that zeolite (sample Z) has shown an optimum removal of mercury than arsenic.

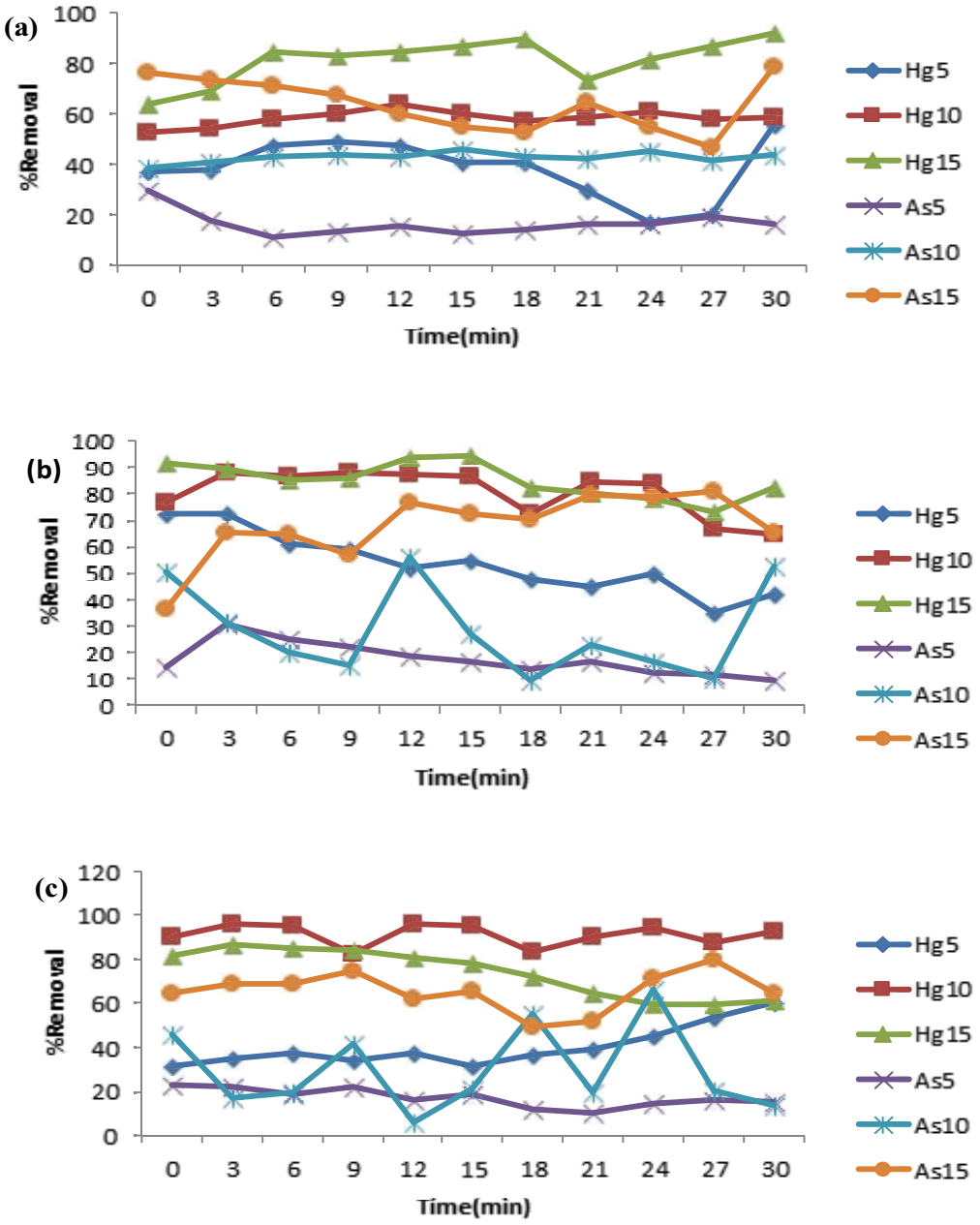

Fig. 4. Removal (%age) of metals on zeolite and metal functionalized hybrids: (a) Z, (b) ZC, and (c) ZZ.

The different dosages of zeolite retained the same preference for adsorption of mercury over arsenic. The higher adsorption of mercury is likely due to its higher molecular weight (MW 200.59) and larger atomic radius (171 pm) that can conveniently make its way to the relatively larger pores in the zeolite matrix [65]. This is strengthened by the fact that the lighter elements are difficult to remove in comparison to heavier elements.

Metal functionalized zeolites also served as adsorbents for the removal of two selected metals as a function of time. It is noted that similar irregular minima to maxima and maxima to minima pattern is observed for Cu-doped and Zn-doped zeolites. However, the former zeolite is more effective in metal uptake than the later. An incremental increase in adsorption is observed with increase in adsorption dosage (from 5 to 15 mg) of metal functionalized zeolite (Fig. 5). It is interesting to note that under all circumstances, mercury is more effectively removed in comparison to arsenic. The minimum and maximum of adsorption for metals depicts the range of 46%–64%, 56%–88%, 66%–96% for Z, ZC, and ZZ, respectively. The functionalization also contributes in the adsorption of metals. The present investigation results clearly indicate that the base material is less efficient for the metal removal than metal hybrids. Increased adsorption capacity for metal is attributed to functionalization [66]. Each adsorbent performs excellent for mercury removal and good for arsenic. The same conclusion is also drawn from the particle size

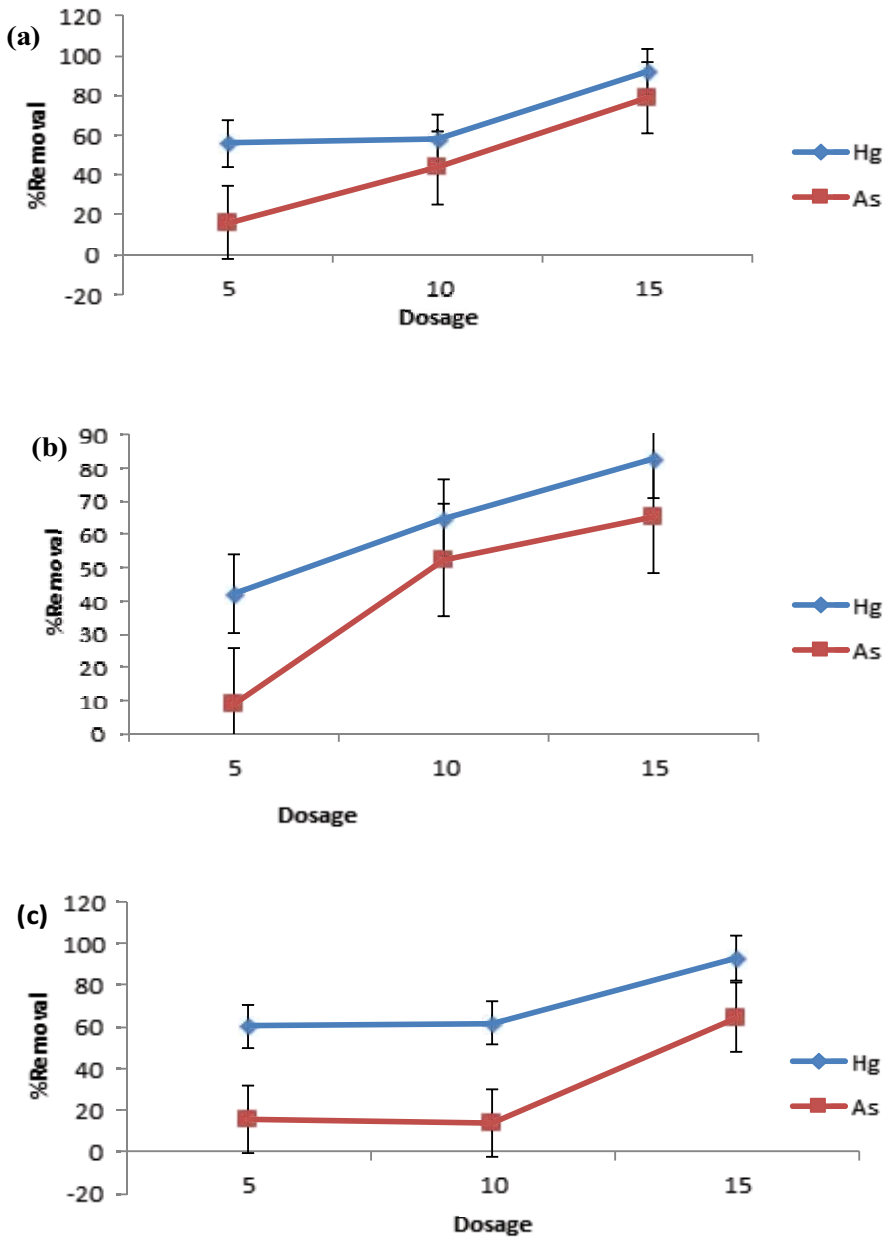

Fig. 5. Effect of dose on removal (%age) of metals on zeolite and metal functionalized hybrids: (a) Z, (b) ZC, and (c) ZZ.

and surface area of synthesized materials. The larger particle size and lesser surface area of zeolite (sample code Z) propose its better removal efficiency for Hg than As.

3.8. Removal of dyes

The synthesized zeolite and its functionalized hybrids are investigated as potential candidates for the removal of dyes. Each member of functionalized hybrid at a fixed dose is applied as adsorbent in closed batch system to remove the known induced concentration of selected dyes (Fig. 6).

Adsorption UV studies when applied on zeolite base material shows removal of Methylene blue and Methyl orange that increase with increase in contact time. The percentage removal calculated for two dyes is comparable and does not vary significantly. On the other hand, percentage removal for two dyes vary to a relatively significant extent in response to metal doped functionalized hybrids. However, Cu- and Zn-doped adsorbents showed better removal for Methyl orange and Methylene blue in respective order.

In addition, hybrid having functionalization of both metals has shown its more potency for Methylene blue removal and it suggests that Zn as counterpart of Cu has more contribution in the removal of dye.

3.9. Adsorption isotherms and kinetics

The experimental data obtained from batch adsorption is treated with Langmuir and Freundlich isotherm models. The results for varying adsorbent doses are summarized

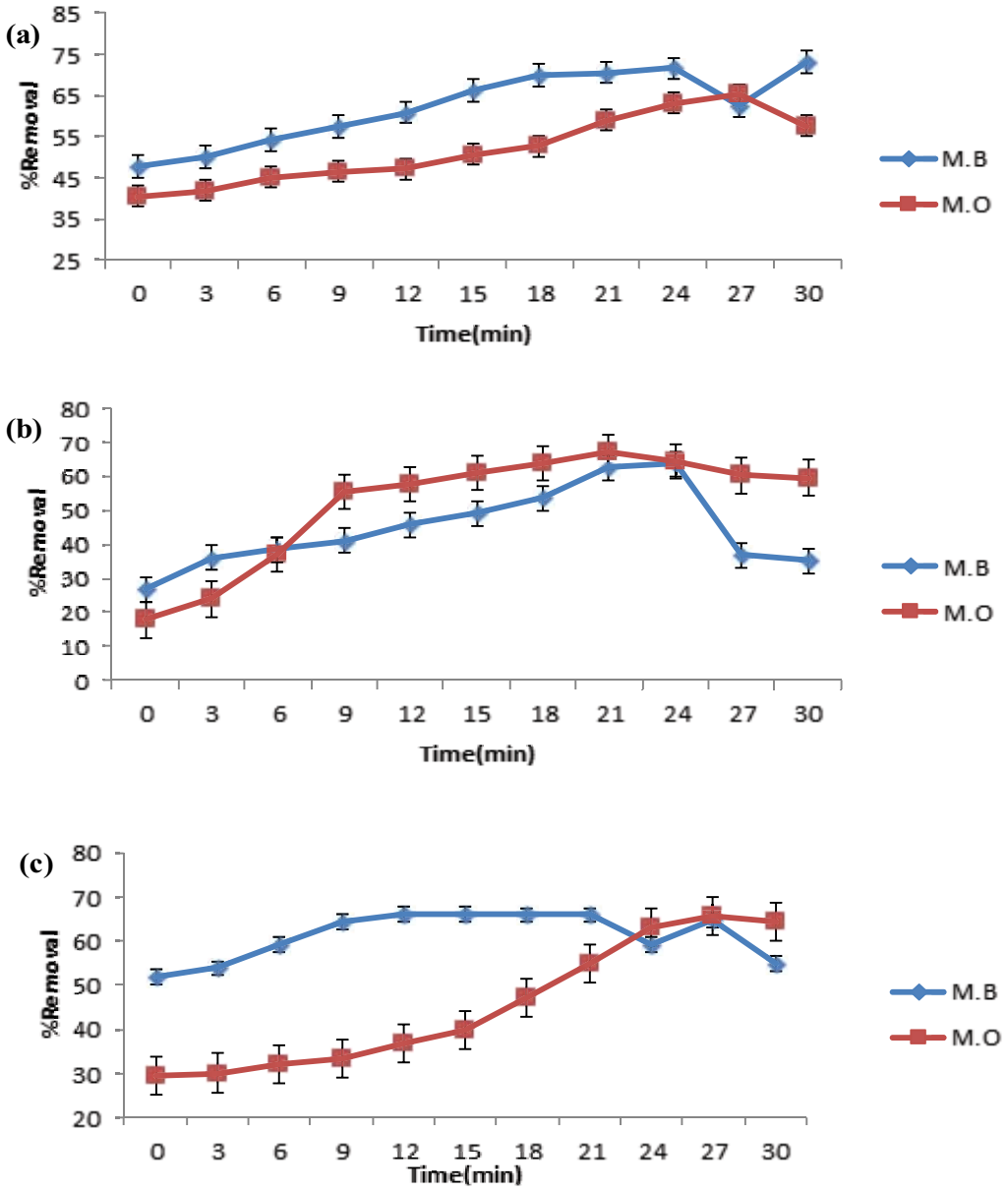

Fig. 6. Removal (%age) of dyes on zeolite and metal functionalized hybrids: (a) Z, (b) ZC, and (c) ZZ.

in Table 4. It is noted that change in adsorbent dose does not have a significant impact on adsorption parameters. Such scenario proposes that synthesized hybrids can be successfully applied as adsorbents in minimum amount (dose) without comprising the efficiency. The economical and green chemistry principles are also considered under the same cover.

The regression coefficient value larger than 0.9 in almost all zeolite based hybrids testifies the fitness of both isotherms. However, zeolite (sample Z) has relatively lower R^2 in comparison to functionalized hybrids, suggesting good contribution of induced functional groups in the zeolite framework. The results are encouraging and determine the efficiency of each synthesized material as good to excellent adsorbent. The fitness of Langmuir and Freundlich to a comparable extent for the removal of mercury and arsenic is attributed to capillary condensation mechanism allowing the sequential uptake of pollutants from sub-monolayer to multilayered structure of adsorbent.

The adsorption efficiency of synthesized materials (zeolites) is determined quantitatively through adsorption kinetics models as well. The results are summarized in Table 5. It is noted that the amount of metal adsorbed (q_e) increases quantitatively with functionalization in comparison to base material. The difference in experimental and calculated q_e is attributed to a number of contributing factors like amount of adsorbent, time of contact, metal salt used and others.

However, mercury is adsorbed more in comparison to arsenic. The result are in conformity with qualitative (removal percentage) adsorption analysis. The regression coefficient (R^2) values reveals the fitness of pseudo-

Table 4
Adsorption isotherm model data for batch experiment of toxic metals on synthesize zeolite hybrids (a) 5, (b) 10, and (c) 15 mg/g.

Hybrid	Langmuir model (Hg)			Langmuir model (Hg)			Freundlich model (Hg)			Freundlich model (As)		
	q_m (mg/g)	K_L (L/mg)	R^2	q_m (mg/g)	K_L (L/mg)	R^2	n	K (mg/g)	R^2	n	K_F (mg/g)	R^2
(a)												
Z	9.54	–0.02	0.90	3.59	–0.02	0.88	–5.04	2.99	0.97	–0.25	1.06	0.95
ZC	28.33	–0.05	0.94	3.07	–0.02	0.86	–1.33	2.12	0.93	–0.23	1.02	0.95
ZZ	19.19	–0.03	0.96	2.56	–0.01	0.93	–0.84	1.76	0.97	–0.19	0.96	0.97
(b)												
Z	33.56	–0.06	0.99	17.64	–0.03	0.996	–12.9	3.26	0.92	–0.73	1.65	0.99
ZC	58.82	–0.22	0.99	6.46	–0.02	0.764	–3.73	2.85	0.97	–0.45	1.35	0.89
ZZ	80.65	–1.29	0.99	6.37	–0.02	0.576	–10.8	3.23	0.95	–0.51	1.44	0.83
(c)												
Z	59.88	–0.25	0.99	38.46	–0.08	0.98	–3.62	2.83	0.97	–1.83	2.37	0.96
ZC	70.92	–0.51	0.99	30.86	–0.06	0.93	–6.85	3.11	0.9	–1.67	2.31	0.89
ZZ	51.28	–0.15	0.99	38.91	–0.08	0.97	–2.88	2.70	0.97	–1.90	2.39	0.94

Table 5
Comparison between the rate constants, q_e, and correlation coefficients associated with the kinetic models for metals at (a) 5, (b) 10, and (c) 15 mg

		Zero-order			Pseudo-first-order		Pseudo-second-order		
Sorbents	Sorbates	$q_{e,(exp)}$ (mg/g)	$q_{e,(cal)}$ (mg/g)	R^2	$q_{e,(cal)}$ (mg/g)	R^2	$q_{e,(cal)}$ (mg/g)	k_2 (g/mg min)	R^2
(a)									
Z	Hg	167.28	123.64	0.08	3.12	0.06	0.04	–59.82	0.634
	As	89.73	71.13	0.07	3.75	0.08	0.06	35.71	0.947
ZC	Hg	219.21	148.36	0.87	2.97	0.87	0.05	–84.14	0.612
	As	75.63	50.994	0.56	4.31	0.53	0.10	–36.57	0.913
ZZ	Hg	180.72	151.69	0.67	2.95	0.66	0.02	234.87	0.851
	As	67.17	45.36	0.55	4.56	0.56	0.07	–13.18	0.999
(b)									
Z	Hg	95.78	39.18	0.17	4.96	0.151	0.02	6.57E-03	0.997
	As	65.49	24.31	0.25	7.08	0.238	0.02	–0.56	0.997
ZC	Hg	132.49	43.43	0.41	4.63	0.399	0.02	–113.68	0.969
	As	78.53	44.70	0.043	4.73	0.026	0.06	–7.27	0.465
ZZ	Hg	139.98	47.54	0.01	4.46	0.018	0.01	0.17	0.992
	As	98.88	68.95	4E-05	3.81	0.002	0.05	27.81	0.413
(c)									
Z	Hg	92.23	18.93	0.39	9.15	0.42	0.01	43.09	0.98
	As	78.67	7.51	0.20	–11.96	0.05	0.01	–7.52	0.89
ZC	Hg	94.56	2.31	0.46	–2.54	0.20	0.01	–64.90	0.99
	As	80.7	25.87	0.45	–1.29	0.68	0.01	40.13	0.97
ZZ	Hg	86.79	–2.54	0.87	–1.44	0.79	0.02	–111.07	0.98
	As	80.17	14.27	0.0006	13.9	0.04	0.02	35.55	0.91

second-order depicting the dependence on adsorbate and adsorbent characteristics for the removal of heavy metals (Hg and As).

Table 5 shows the adsorption kinetics for the removal of Hg and As on different zeolites (adsorbent dose 10 mg). Each of the adsorbent shows preference for the removal

Table 6
Comparison between the rate constants and correlation coefficients associated with the diffusion based rate equations for metals at (a) 5, (b) 10, and (c) 15 mg

		Intraparticle diffusion model			Elovich model	
Sorbents	Sorbates	k_{ip} (mg/g min$^{0.5}$)	C	R^2	β (g/mg)	R^2
(a)						
Z	Hg	–0.35	43.64	0.081	–0.18	0.09
	As	–0.13	18.59	0.07	1.14	0.07
ZC	Hg	–1.11	70.85	0.87	–0.07	0.86
	As	–0.48	24.63	0.56	–0.11	0.97
ZZ	Hg	0.75	29.03	0.67	0.13	0.40
	As	–0.31	21.8	0.55	–0.26	0.51
(b)						
Z	Hg	0.13	56.59	0.17	0.81	0.13
	As	0.09	41.17	0.25	1.29	0.15
ZC	Hg	–0.56	89.06	0.41	–0.12	0.49
	As	–0.36	33.81	0.043	–1.12	0.001
ZZ	Hg	–0.06	92.43	0.015	–0.5	0.08
	As	–0.01	29.92	4.00E-05	0.17	0.05
(c)						
Z	Hg	0.56	73.29	0.39	0.18	0.31
	As	–0.49	71.15	0.21	–0.15	0.21
ZC	Hg	–0.49	92.24	0.46	–0.20	0.28
	As	0.87	54.82	0.45	0.16	0.30
ZZ	Hg	–1.006	89.33	0.87	–0.07	0.79
	As	–0.02	65.9	0.0006	–0.51	0.02

of Hg than As. However, it is interesting to note that with increase in adsorbent dose from 5 mg to 10 mg and 15 mg, the incremental difference in efficiency for the removal of Hg and As reduces. This suggests that higher adsorbent doses are equally good for both metals. Further, fitness of pseudo-second-order kinetics (R^2) is observed for all materials. On the contrary, Elovich and intraparticle diffusion models do not describe the adsorption. This is attributed to the high thickness of the boundary (C value, Tables 4–6), thus limiting the adsorption of the metals approaching the surface.

4. Conclusions

Major conclusions drawn from the study are given below.

The method adopted led to successful synthesis of zeolite based functionalized hybrids. The economical precursor used in synthesis offer advantages of producing thermally stable materials that can work under a wide range of environmental conditions. Further, ratio of Si/Al conveniently places the zeolite in Type A or X class. The incorporation of each functional group is witnessed from FTIR. Cu and Zn exhibited frequencies at 439 cm^{-1} and 418 cm^{-1}. XRD demonstrates the amorphous nature of zeolite framework that generally decreases on functionalization. SEM coupled with EDX portraits the morphological features and elemental composition. The size and molecular weight of induced functional group is the determining factor regarding thermal stability of synthesized material. The BET surface area demonstrates that incorporation of metal plays a significant role in defining the surface area. The batch adsorption experiments confirm the efficiency of synthesized hybrids as adsorbents for the removal of a number of pollutants. In general, mercury showed better removal than arsenic on the adsorbents. The hybrids depict higher removal capacity for Methylene blue in comparison to Methyl orange. The regression coefficient (R^2) values reveals the fitness of pseudo-second-order depicting the dependence on adsorbate and adsorbent characteristics for the removal of heavy metals (Hg and As). The regression coefficient value larger than 0.9 in almost all zeolite based hybrids testifies the fitness of Langmuir and Freundlich isotherms for the removal of mercury and arsenic.

Acknowledgement

The research paper is a part of Ph.D Thesis titled "Development of Functionalized Zeolite Hybrids as Potential Adsorbents" by Noshabah Tabassum that was published on Digital Repository of indigenous literature of Pakistan as per Higher Education Commission of Pakistan degree completion policy. http://173.208.131.244:9060/jspui/handle/123456789/5842.

References

[1] C. Chaffei, K. Pageau, A. Suzuki, H. Gouia, M.H. Ghorbel, C. Masclaux-Daubresse, Cadmium toxicity induced changes in nitrogen management in *Lycopersicon esculentum* leading to a metabolic safeguard through an amino acid storage strategy, Plant Cell Physiol., 45 (2004) 1681–1693.

[2] J. Godt, F. Scheidig, C. Grosse-Siestrup, V. Esche, P. Brandenburg, A. Reich, The toxicity of cadmium and resulting hazards for human health, J. Occup. Med. Toxicol., 1 (2006) 22–22.

[3] L. Järup, A. Åkesson, Current status of cadmium as an environmental health problem, Toxicol. Appl. Pharmacol., 238 (2009) 201–208.

[4] R. Menhage-Bena, H. Kazemian, M. Ghazi-Khansari, M. Hosseini, S. Shahtaheri, Evaluation of some natural zeolites and their relevant synthetic types as sorbents for removal of arsenic from drinking water, Iran. J. Public Health, 33 (2004) 36–44.

[5] S. Shevade, R.G. Ford, Use of synthetic zeolites for arsenate removal from pollutant water, Water Res., 38 (2004) 3197–3204.

[6] V. Somerset, L. Petrik, E. Iwuoha, Alkaline hydrothermal conversion of fly ash precipitates into zeolites 3: the removal of mercury and lead ions from wastewater, J. Environ. Manage., 87 (2008) 125–131.

[7] S.E. Bailey, T.J. Olin, R.M. Bricka, D.D. Adrian, A review of potentially low-cost sorbents for heavy metals, Water Res., 33 (1999) 2469–2479.

[8] F. Fu, Q. Wang, Removal of heavy metal ions from wastewaters: a review, J. Environ. Manage., 92 (2011) 407–418.

[9] F.S. Zhang, J.O. Nriagu, H. Itoh, Mercury removal from water using activated carbons derived from organic sewage sludge, Water Res., 39 (2005) 389–395.

[10] V. Fthenakis, F. Lipfert, P. Moskowitz, L. Saroff, An assessment of mercury emissions and health risks from a coal-fired power plant, J. Hazard. Mater., 44 (1995) 267–283.

[11] T.T. Wałek, F. Saito, Q. Zhang, The effect of low solid/liquid ratio on hydrothermal synthesis of zeolites from fly ash, Fuel, 87 (2008) 3194–3199.

[12] U.K. Chowdhury, B.K. Biswas, T.R. Chowdhury, G. Samanta, B.K. Mandal, G.C. Basu, C.R. Chanda, D. Lodh, K.C. Saha, S.K. Mukherjee, S. Roy, S. Kabir, Q. Quamruzzaman, D. Chakraborti, Groundwater arsenic contamination in Bangladesh and West Bengal, India, Environ. Health Perspect., 108 (2000) 393–397.

[13] M. Vaclavikova, G.P. Gallios, S. Hredzak, S. Jakabsky, Removal of arsenic from water streams: an overview of available techniques, Clean Technol. Environ. Policy, 10 (2008) 89–95.

[14] Y.H. Xu, T. Nakajima, A. Ohki, Adsorption and removal of arsenic(V) from drinking water by aluminum-loaded Shirasu-zeolite, J. Hazard. Mater., 92 (2002) 275–287.

[15] S. Wang, Z. Zhu, Characterisation and environmental application of an Australian natural zeolite for basic dye removal from aqueous solution, J. Hazard. Mater., 136 (2006) 946–952.

[16] G. Crini, Non-conventional low-cost adsorbents for dye removal: a review, Bioresour. Technol., 97 (2006) 1061–1085.

[17] T. Robinson, G. Mcmullan, R. Marchant, P. Nigam, Remediation of dyes in textile effluent: a critical review on current treatment technologies with a proposed alternative, Bioresour. Technol., 77 (2001) 247–255.

[18] S. Wang, M. Soudi, L. Li, Z. Zhu, Coal ash conversion into effective adsorbents for removal of heavy metals and dyes from wastewater, J. Hazard. Mater., 133 (2006) 243–251.

[19] A. Mittal, A. Malviya, D. Kaur, J. Mittal, L. Kurup, Studies on the adsorption kinetics and isotherms for the removal and recovery of Methyl orange from wastewaters using waste materials, J. Hazard. Mater., 148 (2007) 229–240.

[20] M. Rafatullah, O. Sulaiman, R. Hashim, A. Ahmad, Adsorption of Methylene blue on low-cost adsorbents: a review, J. Hazard. Mater., 177 (2010) 70–80.

[21] S. Chen, J. Zhang, C. Zhang, Q. Yue, Y. Li, C. Li, Equilibrium and kinetic studies of Methyl orange and methyl violet adsorption on activated carbon derived from *Phragmites australis*, Desalination, 252 (2010) 149–156.

[22] N. Puvaneswari, J. Muthukrishnan, P. Gunasekaran, Toxicity assessment and microbial degradation of azo dyes, Indian J. Exp. Biol., 44 (2006) 618–626.

[23] M. Elizalde-Gonzalez, J. Mattusch, R. Wennrich, Application of natural zeolites for preconcentration of arsenic species in water samples, J. Environ. Monit., 3 (2001) 22–26.

[24] A. Nishino, Household appliances using catalysis, Catal. Today, 10 (1991) 107–118.

[25] A. Zorpas, T. Constantinides, A. Vlyssides, I. Haralambous, M. Loizidou, Heavy metal uptake by natural zeolite and metals partitioning in sewage sludge compost, Bioresour. Technol., 72 (2000) 113–119.

[26] M. Elizalde-González, J. Mattusch, W.D. Einicke, R. Wennrich, Sorption on natural solids for arsenic removal, Chem. Eng. J., 81 (2001) 187–195.

[27] Y.H. Xu, T. Nakajima, A. Ohki, Adsorption and removal of arsenic(V) from drinking water by aluminum-loaded Shirasu-zeolite, J. Hazard. Mater., 92 (2002) 275–287.

[28] M.S. Onyango, D. Kuchar, M. Kubota, H. Matsuda, Adsorptive removal of phosphate ions from aqueous solution using synthetic zeolite, Ind. Eng. Chem. Res., 46 (2007) 894–900.

[29] A. Wight, M. Davis, Design and preparation of organic-inorganic hybrid catalysts, Chem. Rev., 102 (2002) 3589–3614.

[30] B.Y.S. Al-Zaidi, The Effect of Modification Techniques on the Performance of Zeolite-Y Catalysts in Hydrocarbon Cracking Reactions, Thesis, University of Manchester, 2011.

[31] X. Li, E. Iglesia, Pt/[Fe] ZSM-5 modified by Na and Cs cations: an active and selective catalyst for dehydrogenation of n-alkanes to n-alkenes, Chem. Commun., 5 (2008) 594–596.

[32] L. Guczi, I. Kiricsi, Zeolite supported mono-and bimetallic systems: structure and performance as CO hydrogenation catalysts, Appl. Catal., A, 186 (1999) 375–394.

[33] J. Guzman, B.C. Gates, Supported molecular catalysts: metal complexes and clusters on oxides and zeolites, Dalton Trans., 17 (2003) 3303–3318.

[34] S. Recchia, C. Dossi, A. Fusi, L. Sordelli, R. Psaro, Zeolite-supported metals by design: organometallic-based tin-promoted rhodium/NaY catalysts, Appl. Catal., A, 182 (1999) 41–51.

[35] M. Hartmann, L. Kevan, Substitution of transition metal ions into aluminophosphates and silicoaluminophosphates: characterization and relation to catalysis, Res. Chem. Intermed., 28 (2002) 625–695.

[36] F. Fan, Z. Feng, C. Li, UV Raman spectroscopic studies on active sites and synthesis mechanisms of transition metal-containing microporous and mesoporous materials, Acc. Chem. Res., 43 (2009) 378–387.

[37] Y. Meng, H.C. Genuino, C.H. Kuo, H. Huang, S.Y. Chen, L. Zhang, A. Rossi, S.L. Suib, One-step hydrothermal synthesis of manganese-containing MFI-type zeolite, Mn–ZSM-5, characterization, and catalytic oxidation of hydrocarbons, J. Am. Chem. Soc., 135 (2013) 8594–8605.

[38] G.A. Eimer, L.B. Pierella, G.A. Monti, O.A. Anunziata, Synthesis and characterization of Al-MCM-41 and Al-MCM-48 mesoporous materials, Catal. Lett., 78 (2002) 65–75.

[39] G. Vitale, H. Molero, E. Hernandez, S. Aquino, V. Birss, P. Pereira-Almao, One-pot preparation and characterization of bifunctional Ni-containing ZSM-5 catalysts, Appl. Catal., A, 452 (2013) 75–87.

[40] E. Yuan, W. Han, G. Zhang, K. Zhao, Z. Mo, G. Lu, Z. Tang, Structural and textural characteristics of Zn-containing ZSM-5 zeolites and application for the selective catalytic reduction of NO_x with NH_3 at high temperatures, Catal. Surv. Asia, 20 (2016) 41–52.

[41] M.M. Forde, R.D. Armstrong, C. Hammond, Q. He, R.L. Jenkins, S.A. Kondrat, N. Dimitratos, J.A. Lopez-Sanchez, S.H. Taylor, D. Willock, C.J. Kiely, G.J. Hutchings, Partial oxidation of ethane to oxygenates using Fe-and Cu-containing ZSM-5, J. Am. Chem. Soc., 135 (2013) 11087–11099.

[42] G. Carja, G.Delahay, C. Signorile, B. Coq, Fe–Ce–ZSM-5 a new catalyst of outstanding properties in the selective catalytic reduction of NO with NH_3, Chem. Commun., 12 (2004) 1404–1405.

[43] S. Brandenberger, O. Kröcher, A. Tissler, R. Althoff, Effect of structural and preparation parameters on the activity and hydrothermal stability of metal-exchanged ZSM-5 in the selective catalytic reduction of NO by NH_3, Ind. Eng. Chem. Res., 50 (2011) 4308–4319.
[44] O.D. Ozdemir, S. Pişkin, Zeolite X synthesis with different sources, Int. J. Chem. Environ. Biol. Sci., 1 (2013) 229–232.
[45] S. Özvatan, Y. YÜrÜm, Synthesis of crystalline ZSM-5 type zeolites utilizing primary monoalkylamines 1. Characterization, Energy Sources, 23 (2001) 475–485.
[46] K. Motazedi, Template-Free Synthesis and Modification of LTY, ZSM-5 and LTL Zeolite Catalysts and Investigation of the Catalytic Pyrolysis of Saskatchewan Boundary Dam Coal, Thesis, University of Calgary, 2013.
[47] W. Mozgawa, The influence of some heavy metals cations on the FTIR spectra of zeolites, J. Mol. Struct., 555 (2000) 299–304.
[48] R.M. Alwan, Q.A. Kadhim, K.M. Sahan, R.A. Ali, R.J. Mahdi, N.A. Kassim, A.N. Jassim, Synthesis of zinc oxide nanoparticles via sol–gel route and their characterization, Nanosci. Nanotechnol., 5 (2015) 1–6.
[49] S. Verma, S.L. Jain, Nanosized zinc peroxide (ZnO_2): a novel inorganic oxidant for the oxidation of aromatic alcohols to carbonyl compounds, Inorg. Chem. Front., 7 (2014) 534–539.
[50] I. Markova-Deneva, Infrared spectroscopy investigation of metallic nanoparticles based on copper, cobalt, and nickel synthesized through borohydride reduction method, J. Univ. Chem. Technol. Metall., 45 (2010) 351–378.
[51] V. Parthasarathi, G. Thilagavathi, Synthesis and characterization of zinc oxide nanoparticle and its application on fabrics for microbe resistant defence clothing, J. Pharm. Pharm. Sci., 3 (2011) 392–398.
[52] G. Donny, Synthesis and Characterization of Cu/Ni-Zeolites-A for the Direct Conversion of Methane to Liquid Hydrocarbon, Universiti Malaysia Pahang, Thesis, 2008.
[53] H. Kumar, R. Rani, Structural and optical characterization of ZnO nanoparticles synthesized by microemulsion route, Int. Lett. Chem. Phys. Astron., 19 (2013) 26–36.
[54] S. Cheng, D. Yan, J. Chen, R. Zhuo, J. Feng, H. Li, H.T. Feng, P.X. Yan, Soft-template synthesis and characterization of ZnO_2 and ZnO hollow spheres, J. Phys. Chem. C, 113 (2009) 13630–13635.
[55] Y. Zhang, Y. Zhou, L. Huang, M. Xue, S. Zhang, Sn-modified ZSM-5 as support for platinum catalyst in propane dehydrogenation, Ind. Eng. Chem. Res., 50 (2011) 7896–7902.
[56] A. Hagen, K.H. Hallmeier, C. Hennig, R. Szargan, T. Inui, F. Roessner, State of zinc in MFI type zeolites characterized by XANES and EXAFS, Stud. Surf. Sci. Catal., 94 (1995) 195–202.
[57] B. Notari, Microporous crystalline titanium silicates, Adv. Catal., 41 (1996) 253–334.
[58] S. Srivastava, Synthesis and characterisation of copper oxide nanoparticles, IOSR J. Appl. Phys., 5 (2013) 61–65.
[59] K. Arun, A. Batra, A. Krishna, K. Bhat, M. Aggarwal, J. Francis, Surfactant free hydrothermal synthesis of copper oxide nanoparticles, Am. J. Mater. Sci., 5 (2015) 36–38.
[60] B.E. Alver, M. Sakizci, E. Yörükoğullari, Investigation of clinoptilolite rich natural zeolites from Turkey: a combined XRF, TG/DTG, DTA and DSC study, J. Therm. Anal. Calorim., 100 (2010) 19–26.
[61] M. Sánchez, P. Gamero, D. Cortés, Bioactivity assessment of ZSM-5 type zeolite functionalized with silver or zinc, Mater. Lett., 74 (2012) 250–253.
[62] M. Hassani, G.D. Najafpour, M. Mohammadi, M. Rabiee, Preparation, characterization and application of zeolite-based catalyst for production of biodiesel from waste cooking oil, J. Sci. Ind. Res., 73 (2014) 129–133.
[63] K. Yamamoto, Y. Nohara, Y. Domon, Y. Takahashi, Y. Sakata, J. Plévert, T. Tatsumi, Organic–inorganic hybrid zeolites with framework organic groups, Chem. Mater., 17 (2005) 3913–3920.
[64] R.M.R. Kulkarni, G. Srinikethan, K. Vidyashetty, Equilibrium and kinetic studies for the adsorption of cadmium ion on zeolite 4A, J. Biochem. Technol., 3 (2014) 158–160.
[65] J. Aguado, D. Serrano, J. Escola, J. Rodríguez, Low temperature synthesis and properties of ZSM-5 aggregates formed by ultra-small nanocrystals, Microporous Mesoporous Mater., 75 (2004) 41–49.
[66] I.L. Lagadic, M.K. Mitchell, B.D. Payne, Highly effective adsorption of heavy metal ions by a thiol-functionalized magnesium phyllosilicate clay, Environ. Sci. Technol., 35 (2001) 984–990.